ISSN (Online) 2394-2320

International Journal of Engineering Research in Computer Science and Engineering (IJERCSE)

Vol 10, Issue 4, April 2023

Controlling Fuel Cells with Chaotic Models

[1] Rafael M Gutierrez, [2] Jose L Cruz, [3] Andres I Hernandez, [4] Marie C Pera

[1] New York University Abu Dhabi
[1] [2] [3] Universidad Antonio Nariño
[4] FCLAB
Corresponding Author Email: [1] rmg2165@nyu.edu, [2] jcruz40@uan.edu.co

Abstract*— The Proton Exchange Membrane Fuel Cell (PEMFC) is the most widely fuel cell used today despite its limitations of efficiency and lifetime. Since it has been proven that the PEMFC voltage shows chaotic behavior under certain operating conditions, the development of nonlinear models with chaotic solution should be an important new tool to improve their control and therefore the efficiency, effectivity and pertinent applications of this kind of fuel cells. In this work we propose a procedure to build nonlinear models from time series of the voltage generated by PEMFC at different operational conditions. The procedure starts with a qualitative and quantitative identification of chaotic content of a given time series, continuous highlighting such chaotic content by a feedback procedure of digital filters and ends by capturing and controlling the chaotic behavior with a 3D nonlinear dynamical system with chaotic solutions. When the operation parameters of the PEMFC correspond to a chaotic behavior of the voltage, the fuel cell achieves a robust dynamical equilibrium where the efficiency and durability can be increased.

Index Terms*— Chaos, control, fuel cells, nonlinear dynamics.

I. PROBLEM STATEMENT

Fuel cells have been known since the 19th century with the works of the Welsh physicist Sir William Grove published in 1843 [1]. Fuel cells are energy transforming devices for the hydrogen energy vector, converting chemical energy into electrical energy. There are several types of fuel cells and each type have different functionalities [2]. This article is concerned specifically to the PEMFC (Proton Exchange Membrane Fuel Cell). This type of cell is also the most widely used today, with space travel and the automotive sector being the industries that have made the most use and development of this technology [3]. It has been proven that the PEMFC voltage shows chaotic behavior under certain operating conditions [4]. Therefore, the development of nonlinear models with chaotic solutions [5]-[9], could be an important new tool to improve their control and therefore the efficiency, effectivity and pertinent applications of fuel cells. In this work we propose a procedure to build nonlinear models from time series of the voltage generated by PEMFC at different operational conditions. Initially, many different voltage time series have to be generated corresponding to different operation parameter values. Given the complexity of the system constituted by a PEMFC, the experimental time series of voltage measurements have different sources of dynamical contamination. Therefore, the time series with some potentially useful chaotic content have to be identified, the chaotic content highlighted and finally develop the corresponding nonlinear model.

The procedure starts with a qualitative and quantitative identification of the chaotic content of a given time series using chaotic indicators such as visual inspection of the time series and its power spectrum, estimation of false nearest neighbors, mutual information, maximum Lyapunov exponent and correlation dimension [10]-[12]. Then, the chaotic information content in the identified time series with potentially chaotic behavior has to be highlighted as much as possible in order to separate the chaotic information from other sources of deterministic and stochastic information and contamination. Finally, the chaotic information content of the time series can be used to build a 3D nonlinear dynamical system with chaotic solutions that capture the chaotic dynamics of the fuel cell through its corresponding voltage time series. When the operation parameters of the PEMFC correspond to a chaotic behavior of the voltage, the fuel cell achieves a robust dynamical equilibrium improving its efficiency and durability.

The operation of fuel cells is essentially simple, however, the ideal operating conditions are difficult to obtain and maintain stable during prolonged periods of operation, particularly when the power request presents transients, as is the case in most of applications [13]. The PEMFC is sensitive to variations in the humidity of the membrane, the partial pressure of the reactants $P(H_2)$, $P(O_2)$, the partial pressure of the product $P(H_2O)$ and the temperature T [14], among other variables. A small variation in any of these variables may have strong effects on the general behavior of the PEMFC. A great sensitivity or robustness to internal variables and external perturbations in addition of being a highly nonlinear dynamical system with highly sensitive to initial conditions, implies that under certain conditions the PEMFC may present chaotic behavior, as has been already demonstrated [15]-[16]. Considering that a nonlinear dynamical system with chaotic behavior can be modelled from the measurements of only one of its observables without losing any of the main topological characteristics [17], in principle it would be possible to model

ISSN (Online) 2394-2320

International Journal of Engineering Research in Computer Science and Engineering (IJERCSE)

Vol 10, Issue 4, April 2023

the functioning of a PEMFC by a nonlinear dynamical system with chaotic behavior from its output voltage. The voltage output time series are chosen to identify and capture the chaotic behavior of the PEMFC because it is easy to measure from the fuel cell and it has been observed chaotic content in such time series for certain operational parameter values [15]-[18].

In this work we present a new method to develop a nonlinear autonomous dynamical system as models of the PEMFC in its chaotic operating regime. This method only requires the information contained in the output voltage of the PEMFC. The method is based on time series analysis tools [9] applied in two stages to generated a feedback of new information converging to the optimal model of the corresponding voltage time series. The first stage consists in the qualitative and quantitative selection of potentially useful voltage time series. This selection is performed using the power spectrum, the false nearest neighbors, the maximum Lyapunov exponent and the correlation dimension as indicators and measures of chaotic content in time series [9]. The time series are also detrended and filtered in order to highlight and make a better identification of the chaotic content of each time series. In the second stage, the Takens-Mañe reconstruction theorem [19]-[20], the Gram-Schmidt orthonormalization process, the Adams-Moulton predictor-corrector method [21], and the least squares method are used altogether as an information optimization method to reconstruct the dynamics of the time series in a three-dimensional space. The model obtained in this way is a reconstruction of a dynamical system of nonlinear differential equations in 3D from a scalar time series in 1D [5]. It is considered a reconstruction because it is a dynamical system that generates the trajectory in the 3D state space reconstructed from the scalar time series in 1D. Three independent variables and nonlinear terms of them up to order two are the minimal and sufficient conditions for a 3D nonlinear dynamical model in order to have chaotic solutions [5]-[9].

The digital implementation of the model reconstruction method, is a software tool developed and written in Python language, with all the necessary algorithms to go from the identification of chaos to the reconstruction of the nonlinear dynamical models. We call this software CMRTS, Chaotic Model Reconstruction from Time Series. CMRTS was applied to different voltage time series as the outputs of a PEMFC with different operational parameter values obtaining interesting results that indicate a potential chaotic dynamical stability for some of them.

This article is organized as follows: Section 2 presents in detail the method applied for the reconstruction of 3D nonlinear dynamical systems models with chaotic solutions from scalar time series in 1D, and the software developed to implement the method described. Section 3 presents the application of the method to a voltage time series from a PEMFC at different operational conditions, to obtain a nonlinear dynamical model of its chaotic behavior. In Section 4 are presented and discussed the results obtained in the previous section. Section 5 presents conclusions and prospects for future work.

II. THEORETICAL FRAMEWORK

The operation of the PEMFC can be seen in a simple way. Hydrogen feeds the anode and decomposes into an electron and a proton, the electron passes through a circuit, while the proton passes through the membrane of the PEMFC, in the cathode the electron and the proton are recombined forming the hydrogen atom again, closing the electrical circuit and reacting with the oxygen or air feeding the cathode to form water molecules and heat, as shown in the balance of equation (1) [13]:

$$4H^+ + 4e^- + O_2 \rightarrow 2H_2O + heat \qquad (1)$$

Although its operation is essentially simple, ideal operating conditions are difficult to obtain and maintain for long periods of time [14]. This is due to the fact that the optimum operation condition is obtained for high reactant pressures, low product partial pressures, and low ohmic membrane resistance, this last obtained for high levels of water content in the membrane. Under these conditions, the system is unstable, a fully humidified membrane can easily derive into a flooded cathode affecting reactant partial pressures in the cathode and degrading the fuel cell performance. On the other hand, slight variations in temperature or cathode gas flow and humidity content can easily either flood the cathode or dry the membrane, both, considered non-optimal operation conditions. In most operation conditions, power transients and power control systems, will cause variations in current, voltage, temperature, gas flow, and gases partial pressures, making very difficult for the system to remain in the optimum operation conditions for each power demand. In consequence, it is necessary to have an optimum control of these parameters using monitoring and diagnostic techniques [15]. Some of the techniques most used in the diagnosis of PEMFC are based on the construction of models of their operation for the detection of faults [16].

The PEMFC models are divided into two main branches, the analytical or white box models and the black box models, there is also an intermediate branch called grey box models which is a mix between the white box models and the black box models. The white box models are based on the construction of differential equations that simulate the ideal behavior of the PEMFC and failures are diagnosed when the real behavior of the PEMFC differs greatly from its ideal behavior. This type of model is very efficient in finding faults in the operation of the PEMFC. However, due to the complexity of the behavior of the PEMFC, these models relate a number of variables that significantly increase the

ISSN (Online) 2394-2320

International Journal of Engineering Research in Computer Science and Engineering (IJERCSE)

Vol 10, Issue 4, April 2023

time required to solve the equations and make it difficult for this type of model to be used to diagnose faults online. The black box models solve the aspect of the execution time, these models are created from the existing correlations between the input and output data, therefore, no additional information is required of the internal operation of the PEMFC, significantly reducing the number of variables and relationships to consider, this implies a reduction in the time spent in the construction and evaluation of the models. These types of models are best for online fuel cell diagnostics. However, since they are based on input and output relationships, they lose generality when applied to PEMFC with different characteristics. The most used methods in this type of model are neural networks, fuzzy logic and vector support machines. On the other hand, there are the grey box models that largely solve the calculation times presented by the models of white box reducing the number of variables with which it works. The most common way to reduce variables is to find correlations from data taken from the PEMFC, however, as the number of variables is reduced, the generality of the models is lost [13]-[16] and [18].

This article presents a novel method to create a combination of white and black box models of PEMFCs under chaotic behavior conditions when stability and robustness may be expected by the nature of such behavior of complex systems. The method initially uses indicators of nonlinear information content in time series such as the power spectrum, mutual information, false nearest neighbors, Lyapunov exponents, and dimension correlation to identify the possible chaotic behavior of the PEMFC voltage time series. Since real time series always have different sources of low and high frequency contamination, a diversity of bandwidth filters is applied to highlight the chaotic content of the time series; this procedure is guided by the tendencies of the nonlinear indicator just mentioned. The reconstruction or construction of the model by means of a 3D trajectory reconstruction from a 1D time series, is the reconstruction of the attractor that represents the dynamics of the system in the 3D phase space, it is the trajectory in the state space of the system. This procedure is performed based on the Takens-Mañe reconstruction theorem as the demonstration that all the dynamical information of the three variables of a 3D nonlinear dynamical system can be extracted from a time series of only one of the variables. Then, it is defined a measure in state space and the Gram-Schmidt orthonormalization process is applied to build an orthonormal polynomial base up to order two, and finally the Adams-Moulton method and the least squares method are used to estimate the values of the polynomial coefficients consistently with the information contained solely in the original time series. These stages are described in more detail in subsections *A* and *B*.

A. Identifying chaos in time series

Most complex systems must have nonlinearities that represent feedbacks and other dynamical diversity and richness of their dynamics, and these nonlinearities may produce chaotic behavior. However, diverse sources of contamination present in any real time series may hide its chaotic content. This constitutes an important challenge: detection and highlight the chaotic content of a real time series of measurements to better understand the dynamical information and properties of the system it represents. To determine if a time series contains a possible chaotic behavior and highlight it from diverse sources of contamination, several measures of chaos are used as they are mentioned and organized in Figure 1.

First, the power spectrum is a powerful tool of time series analysis that allows us to observe important qualities of the dynamics of the system contained in the corresponding time series: if a time series is completely stochastic, its spectrum is characterized by a continuous distribution in a very wide range of frequencies without distinguishing any particular preference in any specific frequency or range of frequencies; if the time series corresponds to a linear deterministic system, its solutions are periodic and the spectrum shows well-defined peaks at specific frequencies and their harmonics; finally, if a time series contains deterministic chaos information, the power spectrum shows an energy distribution at various frequencies, almost continuous and rapidly decreasing in a defined range with a certain structure, and the amplitude must be very low both at very low frequencies that represent trends and non-stationarity, and at high frequencies that represent contamination with high-frequency white noise. In this way, the power spectrum serves as a qualitative method of analysis to determine the potential for chaotic content that the time series may have. If the power spectrum indicates weak but interesting chaotic content with low and/or high frequency noise, in each case various low-pass, high-pass or band-pass filters can be applied as a first feedback process to identify, highlight and verify the chaotic content of the time series.

Second, the false nearest neighbors' method, FNN [6], uses the correlation of the time series data at increasing dimensions, to identify the minimum dimension that the attractor must have according to the deterministic chaos information it contains. The number of false neighbors must be reduced as the dimension increases until it tends to zero in the appropriate dimension for ideal time series or to a low asymptote when acceptable contamination remains. The remaining value of FNN for high dimensions is a good indicator of the noise or high frequency contamination of the time series that may be filtered out appropriately to highlight the chaotic content of the time series [5]-[12].

Third, the Lyapunov exponents, and more precisely the maximum Lyapunov exponent [6]-[10], is a measure of the sensitivity to the initial conditions of the system, measuring

ISSN (Online) 2394-2320

International Journal of Engineering Research in Computer Science and Engineering (IJERCSE)

Vol 10, Issue 4, April 2023

the divergence between nearby trajectories in phase space which increases exponentially for chaotic behavior. For a time series the maximum Lyapunov exponent can be numerically estimated with high accuracy depending on the purity of the data. If the maximum Lyapunov exponent is positive, it is good indicator of chaotic behavior. In a *n*-dimensional dynamical system, each of the *n* dimensions has its own Lyapunov exponent. For a 3D dynamical system, chaos occurs when there is one positive, one zero and one negative exponent [10]-[12].

Finally, a chaotic attractor defining the trajectory of the dynamical system in the 3D state space, must have a non-integer or fractal dimension. The dimension of the phase space where the attractor exists, is the integer dimension immediately greater than the dimension of the attractor. There are several numerical methods and measures to estimate the dimension of the attractor from a time series from different practical definitions of the attractor dimension, but the most representative and used for real time series, is the dimension of correlation measure [5]-[12].

No one of these four or any other indicator of chaos content in a time series by itself is a sufficient and definitive evidence of chaos in a specific time series, depending on the characteristics of the time series one indicator alone can be fooled in one way or the other. However, used together, the four indicators can give reliable results. As it was already mentioned, due to the noise generated by sampling measurements in real time series, in most of the cases its potential chaotic content cannot be clearly isolated. It is necessary an initial filtering process of the time series, not only to highlight the possible chaotic content, but to improve the modelling results that become another important source of information by feedback between the empirical, theoretical and numerical information of the corresponding dynamical system. There are different techniques for time series filtering, depending on the characteristics of the noise and other sources of contamination present in the time series which are not very well known and only partially controlled experimentally. In general, it is advisable to have some prior knowledge of the behavior of the dynamical system under study, to avoid eliminating relevant data or adding artificial information that does not correspond to the behavior of the original time series during the filtering process [5]-[12].

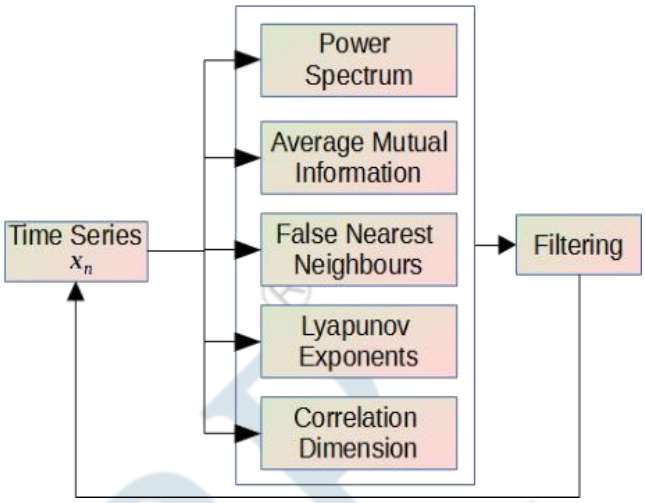

Figure 1. Filtering pre-process applied to fuel cell voltage time series to detect and highlight potential chaotic behavior.

B. Construction of models

The modelling method is based in the procedure indicated in initially and further developed for climate measurements [5]. The obtained models are autonomous nonlinear dynamical systems of differential equations of polynomials up to second order in three variables, with trajectory solutions in the corresponding 3D state or phase space as shown in equation (2) [5]:

$$\dot{\vec{x}} = F_{\vec{x}}(\vec{x}) = \overrightarrow{C_{\vec{x}}} \cdot \Pi^I(\vec{x}), \tag{2}$$

where $\vec{x} = (x, y, z)$ is the state vector in 3D defining the trajectory of the system as the solution of the dynamical system. $\overrightarrow{C_{\vec{x}}}$ is a coefficient vector of three elements and $\Pi^I(\vec{x})$ indicates the polynomials in three variables with all the nonlinearities up to order two as shown in equation (3). The elements of $\overrightarrow{C_{\vec{x}}}$ determine the contribution of each polynomial to the dynamical system. Therefore, the product of the right-hand side of equation (2) generates a matrix of coefficients with 30 elements: ten for each variable corresponding to one constant term, four linear terms and six nonlinear terms as all possible nonlinearities up to order two among three variables. $I = (i, j, k)$ is the vector index of the ten polynomials $\Pi^I(\vec{x})$, varying from $(i, j, k) = (0,0,0)$ to $(i, j, k) = (2,2,2)$, with the constraint $k \leq j \leq i$:

$$\Pi^{(i,j,k)}(\vec{x}) = \sum_{h=0}^{i-1}\sum_{g=0}^{h}\sum_{f=0}^{g} \alpha_{fgh}^{(i,j,k)} x^{h-g} y^{g-f} z^{f} + \sum_{g=0}^{k}\sum_{h=0}^{j-g} \eta_{gh}^{(i,j,k)} x^{i-h-g} y^{h} z^{g} \tag{3}$$

In order to avoid data overlap between the terms of the polynomial base $\Pi^I(\vec{x})$ and guarantee the efficiency of the representation of the trajectory, the polynomials must be linearly independent and normalized over the discrete

ISSN (Online) 2394-2320

International Journal of Engineering Research in Computer Science and Engineering (IJERCSE)

Vol 10, Issue 4, April 2023

measure defined in the state space, i.e. an orthonormal base. The Takens-Mañe reconstruction method [18]-[19] is initially used to convert the 1D time series into a 3D trajectory in state space representing each point of the trajectory by the 3D vector $(x, y, z) = (x_n, x_{n+\tau}, x_{n+2\tau})$ where x_n is the original 1D time series and τ is the reconstruction delay time estimated by using the mutual information theory [6]. The Gram-Schmidt orthonormalization process is applied to obtain the necessary orthonormal base from the general polynomial expression of equation (3).

The coefficients of $\overrightarrow{C_{\vec{x}}}$ and the orthonormal base $\Pi^I(\vec{x})$ in the right side of equation (2) are estimated using the Adams-Moulton corrective predictor method and the least squares method with an information optimization processes that allows to maximize the capture of the chaotic content of the time series avoiding as much as possible the contamination sources. The Adams-Moulton method basically performs a numerical integration as a predictor of the function that represent the dynamics of the reconstructed vector using the past information as shown in equation (4):

$$\vec{x}_{n+1} = \vec{x}_n + \Delta t \sum_{j=0}^{M} a_j^{(M)} F_{\vec{x}}(\vec{x}_{n+1-j}) \qquad (4)$$

where $\vec{x}_n$ is the *n*-th term of the reconstructed vector, Δt is the time elapsed between two successive measurements of the reconstructed trajectory in 3D, M is the number of previous steps used to make the correction of the prediction and $a_j^{(M)}$ are the Adams coefficients already defined for various values of M in [5] and [21]. Replacing $F_{\vec{x}}$ from equation (2) into equation (4) we obtain the following expression (5):

$$\left(\sum_{j=0}^{M} a_j^{(M)} \Pi^I(\vec{x}_{n+1-j})\right) \cdot \overrightarrow{C_{\vec{x}}} = \frac{\vec{x}_{n+1} - \vec{x}_n}{\Delta t} \ . \qquad (5)$$

Since the matrix of coefficients is not a square matrix, the Moore-Penrose pseudo-inverse is used to solve the system of equations:

$$\vec{x} = A^{\dagger}\vec{b}$$

where the symbol † denotes a pseudo-inverse [5], then we obtain equation (6) where $\Delta\vec{x}_n = \vec{x}_{n+1} - \vec{x}_n$ and the $\vec{C}_{\vec{x}}$ are the coefficients determined by:

$$\vec{C}_{\vec{x}} = \left(\sum_{j=0}^{M} a_j^{(M)} \Pi^I(\vec{x}_{n+1-j})\right)^{\dagger} \cdot \frac{\Delta\overrightarrow{x_n}}{\Delta t} \qquad (6) \qquad (6)$$

The model in equation (2) is then completely determined since the polynomials $\Pi^I(\vec{x})$ are known and $\overrightarrow{C_{\vec{x}}}$ have numerical well-defined values for a specific time series. Finally, the Runge-Kutta numerical integration method is used to integrate equation (2) with all the values of the parameters using one-time steps and 10000 iterations to display the solutions of the obtained dynamical systems. The final result is the trajectory of the system in the 3D state space of variables *x*, *y* and *z* corresponding to a particular time series as will be presented in the following sections.

C. Software CMRTS

As already indicated, CMRTS is for Chaotic Model Reconstruction from Time Series, a software developed by the authors for the reconstruction of nonlinear models with chaotic behavior from a time series [5]. This software is written in Python and covers the model reconstruction and analysis methods described in subsections *A* and *B*. In addition, CMRTS has a graphical user interface divided into three main parts: Model, pre-process and process, as shown in Figure 2.

The Model section of CMRTS allows the user interaction with the obtained models for a particular time series. It allows the integration of the models using the Runge-Kutta method, the control of the parameters such as the integration step and the desired number of iterations in each different integration. It also has diverse visualization tools for visual inspection and analysis of the trajectories generated by the integration of the obtained models.

The Pre-process section of CMRTS is focused on verifying the chaotic content of the time series, using chaos measures. In this section the software tool calculates, graphically and numerically: The mutual information, the power spectrum, the false nearest neighbours, the Lyapunov exponents and the correlation dimension, which are altogether necessary and sufficient to evaluate the chaotic content of the time series as described in subsection *A*. This section of CMRTS also allows the application of digital filters, detrending and smoothing procedures to highlight the chaotic content of a time series.

The Process section of CMRTS is where the construction of the models takes place. This section implements, in a transparent way for the user, the Takens-Mañe reconstruction theorem, the Gram-Schmidt orthonormalization process, the Adams-Moulton prediction-correction method and the least squares method, described in subsection *B* for model reconstruction. In addition, the reconstruction time τ can be varied in such a way that several models can be built from a single time series for subsequent evaluation using the Model section.

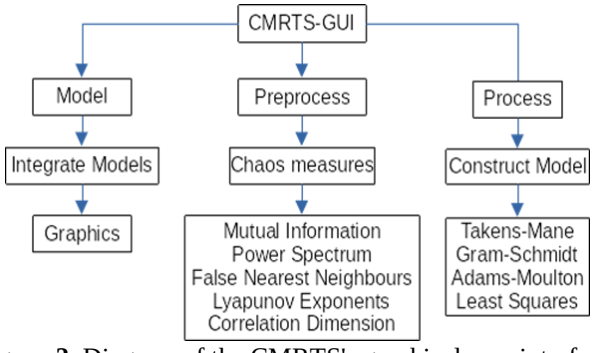

Figure 2. Diagram of the CMRTS's graphical user interface, specifying the different functionalities and the corresponding processing sequence.

ISSN (Online) 2394-2320

International Journal of Engineering Research in Computer Science and Engineering (IJERCSE)

Vol 10, Issue 4, April 2023

III. METHODOLOGY

The experiments necessary to detect and model chaos in the voltage time series from PEMFC were carried out in the specialized laboratory FCLAB, a technical and scientific resource center dedicated to systems in the Hydrogen-Energy sector in France. A test bench with gas inlet and purge valves was used in a ZSW brand fuel cell composed of five square cells, with an effective area of 100cm^2 to obtain the time series of voltage measurements. The fuel cell was tested for the conditions stated in Table 1. Due to the difficulty of controlling and keeping stable the relative humidity *RH* of the membrane, it was fixed at 70% for all experiments. These values were chosen considering that the chaotic behavior in PEMFC tends to occur in extreme conditions, in particular near flooding conditions, when the *RH* is high, close to 100% and the H_2 stoichiometry is near 1, temperature *T* around 50°C and current density *J* in approximately equal to 1 in the units indicated in Table 1. The experiments were carried for the 27 combinations of the values of variables in Table 1, with a sampling rate of 5 samples every 3 seconds, for a period of time of 15 minutes. From this procedure, 27 time series of the fuel cell voltage were obtained, each with 1500 data points. The obtained time series were tested for chaotic behavior as presented in section *A*. The procedure was executed by the CMRTS software described in subsection *C*. The voltage time series that showed more indications of possible chaotic behavior as mentioned before, were selected and the results analyzed.

Table 1

RH	$T(°C)$	Sto	$J(A/cm^2)$
~70%	50	1,1	0,8
	55	1,3	0,9
	60	1,5	1

Table 1. Design of experiments to detect deterministic chaos in the PEMFC voltage: the temperature *T*, the hydrogen stoichiometry *Sto* and the current density *J* are varied, each one in three different values, obtaining 27 combinations of parameter values.

We then proceed to pre-process and process the time series to build the models of the corresponding systems with the selected time series in the previous step. This procedure also runs on the CMRTS software. The procedure starts with the 3D reconstruction in the phase space of each of the voltage time series using the Takens-Mañe theorem. The time delay τ was varied from 1 to 200 times Δt, obtaining 200 reconstructions for each time series and subsequently the same number of models to evaluate. The orthonormal polynomial base is obtained applying the Gram-Schmidt process to the reconstructed 3D trajectory. The coefficients of the model $\overrightarrow{C_{\vec{x}}}$, are obtained using the Adams-Moulton method and the Moore-Penrose pseudoinverse. The Adams-Moulton method is used as shown in equation (4) of subsection *B* with a number of previous steps $M = 3$ to correct the prediction of the values of $F(\vec{x})$ considering the reconstructed vector $\overrightarrow{x_n}$, as can be seen in equation (5); larger and smaller values of *M* were not consistent with the considered time scales and sampling frequency as the results obtained made it evident. The Moore-Penrose pseudoinverse is then used as shown in equation (6). Finally, having the orthonormalized polynomial base and the coefficients already determined, these two factors are multiplied and a model is obtained as shown in equation (2).

It should be noted that with this procedure the models are built exclusively using experimental data, without the need of any other information apart from that contained in the fuel cell voltage signal time series. It is also important to note that after this modelling procedure, only a few of the thirty coefficients of the general model for a 3D nonlinear autonomous dynamical system of polynomials up to order two, get significant values different from zero, obtaining in this manner a relatively very simple model of a very complex dynamics thanks to the nonlinearities and deterministic chaos of nonlinear models.

Finally, the fourth order Runge-Kutta method is applied to integrate the obtained models, using an integration step $h = 0.001$, with 10000 iterations and initial conditions $(x_0, y_0, z_0) = (x_1, x_{1+\tau}, x_{1+2\tau})$, where x_1 is the first data of the voltage time series being modelled. The integrated models are evaluated, initially by visualisation selecting those that present a chaotic solution describing a qualitatively fractal attractor. Additionally, using the chaos measures described in subsection *A*, the most promising models are selected using the feedback provided by the pre-processing indicated before to highlight the chaotic content in real contaminated time series. The CMRTS makes easy to try different time series, parameter values and models, nimbly performing tries and errors to find the optimal conditions and converge to the optimal model for a given time series.

IV. RESULTS

From the 27 experiments proposed in Table 1, it was possible to obtain good voltage data time series for only 19 of them. For the remaining 8 experiments the PEMFC control system was automatically activated stopping the operation for security reasons of the fuel cell. The corresponding 19 voltage time series were visually analyzed and estimated the chaos content of each one with the chaos measures described above. Table 2 shows the results of 19 time series with the corresponding PEMFC operation parameter values. N_{Test} is the identifier for each experiment, *T* is the temperature of the stack, *Sto* the anode stoichiometry, *J* the current density and *RH* is the relative humidity of the membrane. *PS* refers to the power spectrum as a visual qualitative measure, then "Y" indicates a clear potential chaotic content of the time series,

ISSN (Online) 2394-2320

International Journal of Engineering Research in Computer Science and Engineering (IJERCSE)

Vol 10, Issue 4, April 2023

otherwise it is marked with "N". The τ is the delay time obtained from the mutual information, *FNN* is the estimate of the minimum dimension in which it is possible to unfold the attractor, *Lyap* is the maximum Lyapunov exponent indicating sensitivity to the initial conditions when positive, *CD* is the correlation dimension indicating a strange attractor when its value is not integer.

Table 2

N_{Test}	*T*	*Sto*	*J*	*RH*	*PS*	τ	*FNN*	*Lyap*	*CD*
1	50	1,3	0,8	75	N	24	4	0	6,23
2	50	1,3	0,9	73	N	25	4	0	9,11
3	**50**	**1,3**	**1**	**76**	**Y**	**4**	**3**	**0,11**	**6,63**
4	50	1,5	0,9	80	N	18	4	0	1,17
5	50	1,5	1	76	N	16	4	0,07	8,29
6	**55**	**1,1**	**0,8**	**74**	**Y**	**12**	**3**	**0,31**	**7,49**
7	55	1,3	0,8	70	N	29	4	0,06	7,60
8	**55**	**1,3**	**0,9**	**65**	**Y**	**8**	**3**	**0,10**	**6,80**
9	55	1,3	1	60	N	21	5	0	7,93
10	55	1,5	0,8	68	N	39	5	0	8,62
11	55	1,5	0,9	82	N	18	4	0	6.00
12	55	1,5	1	75	N	17	4	0,09	4,15
13	60	1,1	0,8	65	N	4	4	0,06	5,73
14	**60**	**1,3**	**0,8**	**67**	**Y**	**4**	**3**	**0,06**	**5,62**
15	**60**	**1,3**	**0,9**	**69**	**Y**	**5**	**3**	**0,04**	**5,91**
16	60	1,3	1	67	N	20	3	0,22	2,71
17	60	1,5	0,8	72	N	x	x	x	x
18	60	1,5	0,9	57	N	7	4	0,05	7,36
19	60	1,5	1	73	N	7	4	0,07	4,39

Table 2: The 19 time series of the corresponding experiments with its operation parameter values and chaos measures. N_{Test} is the number that identifies the selected experiment, T is the temperature of the cell, *Sto* is the anode stoichiometry, J is the current density, RH is the Relative Humidity of the cell, PS is the Power Spectrum, τ is the time delay, FNN are the False Nearest Neighbors, *Lyap* is the largest Lyapunov exponent and *CD* is the Correlation Dimension.

These measures used as indicators of possible chaos content in the time series cannot be conclusive because of many reasons, in particular for the finite resolution of the data points, sampling frequency and time span of observation. Formally and rigorously, the results would not be conclusive for each measure independently even if the data would have infinite resolution, infinite sampling frequency or continuous measurement and practically infinite observation time span. However, for some real time series it has been observed rapid convergence to conclusive results although, the omnipresent contamination from diverse sources that makes necessary the coherent interpretation of the imprecise and qualitatively results of the application of several chaos measures as proposed in this work.

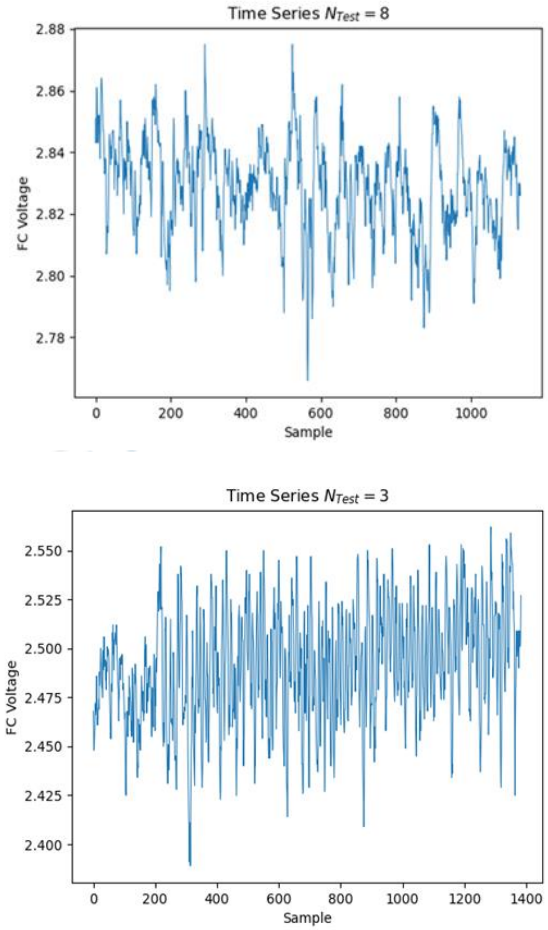

Figure 3. Voltage time series of the experiments 3 and 8, top and bottom respectively.

The five experiments, N_{Test} *=3,6,8,14 and 15*, are highlighted in Table 2 to indicate that they have the most promising measures indicatives of highly possible chaotic behaviour and the cases with the smaller value of FNN equal to *3*. For these five experiments, the time lag τ has the smaller values indicating that the nonlinear correlations are not very large indicating stochastic or noise dominated time series; the

ISSN (Online) 2394-2320

International Journal of Engineering Research in Computer Science and Engineering (IJERCSE)

Vol 10, Issue 4, April 2023

maximum Lyapunov exponent *Lyap* are positive and small but significative indicating sensitivity to initial conditions, however the experiments *14* and *15* have very small values reducing the possibility of chaotic content. Finally, the correlation dimension *CD* results are high, indicating potential chaotic content but highly contaminated, also indicated by the remaining tendency of the FNN as can be seen in Figure 5. In these experiments the most recurrent operation parameter is the stoichiometry equal to *1.3*, the other operation parameters do not have a clear predominant value although the variations are small as was indicated before in the planning and design of the experiments.

Accordingly, with the mentioned results, the time series corresponding to the experiments 14 and 15 seem to have no much more information than noise of a small relative voltage amplitude, ~0.05, with a large relative voltage peak of ~0.25. The time series of experiment 6 shows a very small relative noise with a few very large peaks indicating a very unstable operation with very low potential to have chaotic content.

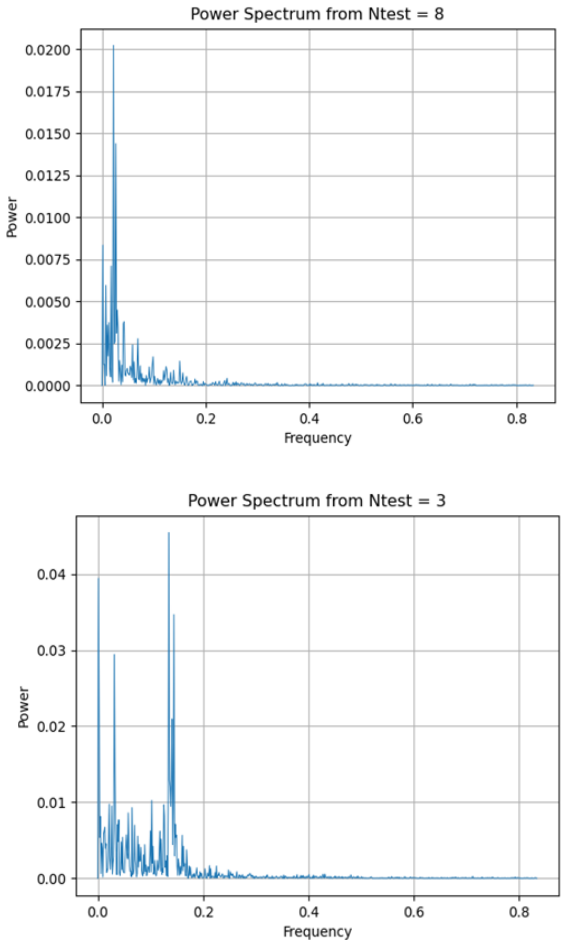

Figure 4. Power Spectrum for experiments 3 and 8, top and bottom respectively.

Therefore, we are going to continue the analysis and modeling of only these two time series corresponding to the experiments, $N_{Test} = 3$ *and 8*, the only ones with significative possible chaotic content so far. However, all calculations and proofs are going to be performed for all the nineteen time series for the sake of comparisons when useful and illustrative. The two corresponding power spectrums, presented in Figure 4, show a range of frequencies small and continuously decreasing amplitude from low to higher frequencies which is a good initial indicator of chaotic content in the time series. However, for $N_{Test} = 3$ there are two trouble features: there is a very high amplitude for very low frequencies indicating a strong trend of the time series as a source of contamination, and a large and wide second pick for relatively high frequencies indicating both contaminations from a periodic signal and medium to high frequency noise. These two sources of contamination can hide the chaotic content of the time series. In the case $N_{Test} = 8$, the nonstationary or low frequency contamination is weaker and the second peak is not present.

Figure 5 shows the FNN of experiments 3 and *8*. The relative slow decrease from imbedding 1 to 2, then a faster decrease from embedding 2 to 3 and finally slower decrease for larger embedding, very similar for the two time series. This is a good indicator of chaotic content with a potential embedding dimension closer to 3 than to 4 with a reasonable noise contamination. In the case of a stochastic or very noisy time series the FNN would give a very fast decrease from embedding 1 to 2 and a remaining small oscillating amplitude for larger embeddings.

Filtering a time series with chaotic content is a very tricky process because we do not know *a priory* how much chaotic power is contained in each frequency of the power spectrum. We only know that the chaotic information is mostly contained in a wide range of medium frequencies and is very difficult to disentangled it from contamination sources without effecting the chaotic content by deleting or aggregating some valuable and delicate information in the filtering process. However, we know that outside the "chaotic range" of frequencies, i.e. towards low and high frequencies, nonstationary sources of information and white noise respectively, are dominant. The challenge with digital filters is the correct definition of the high pass and low pass frequencies and their strength within the frequency "chaotic range". A first approximation to solve this problem without affecting much the chaotic information content of the time series can be performed by successively remove the linear tendency of the time series as a soft high pass filter and applying a local discrete gaussian average as a soft binomial low pass filter. As already mentioned and consistently done with the power spectrum results, the two time series from experiments *3* and *8*, have small but important linear tendencies to be removed, increasing and decreasing respectively as can be observed in Figure 3. These tendencies can be easily removed by fitting the time series to a straight line with a minimum square method and subtracting the

ISSN (Online) 2394-2320

International Journal of Engineering Research in Computer Science and Engineering (IJERCSE)

Vol 10, Issue 4, April 2023

corresponding value to each data point of the time series. In order to remove the high frequency noise contamination, each data point of the time series is replaced by the mean value with its four nearest neighbour data points weighted by the coefficients of Pascal's triangle:

$$x_i^f = \frac{1}{16}(x_{i-2} + 4x_{i-1} + 6x_i + 4x_{i+1} + x_{i+2})$$

where x_i^f is the *i*-th filtered data point of the time series. Since these two procedures are linear, they can be applied in any order with the same results aside of small variations from numerical precision as can be seen in Table 3, where are presented the results of the nonlinear measures for the time

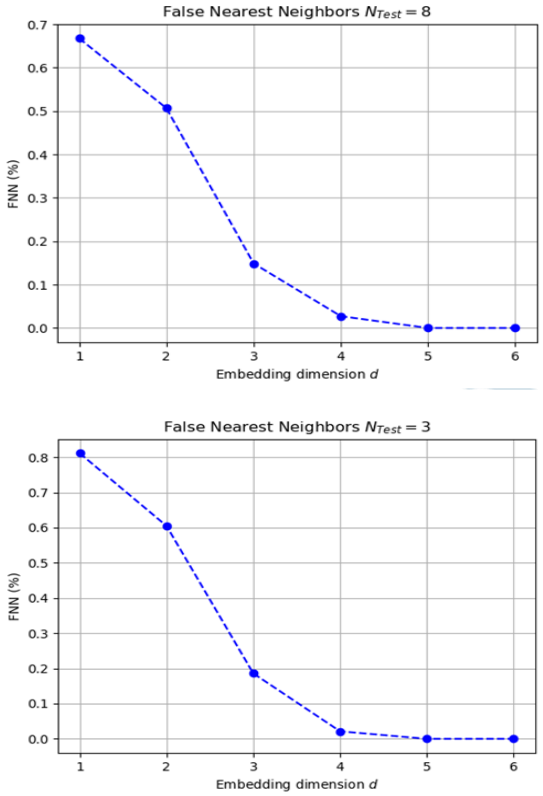

Figure 5. False Nearest Neighbors, FNN, for the two time series of experiments N_{Test} = 3 and 8, top and bottom respectively.

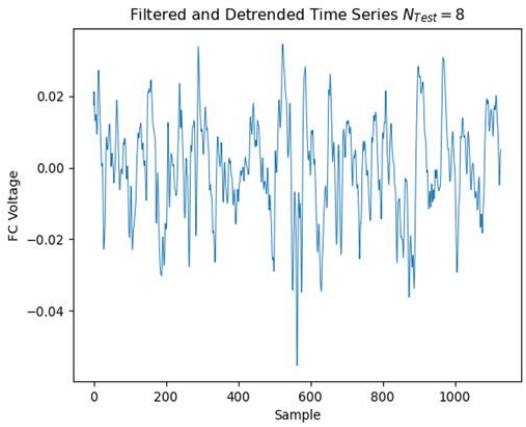

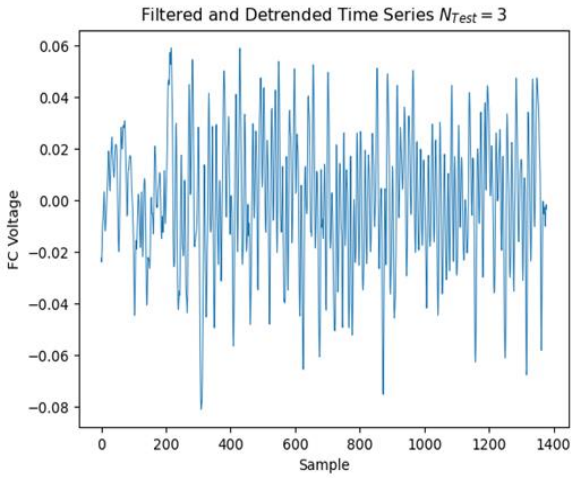

Figure 6. Time series corresponding to experiments N_{Test} = 3 and 8, top and bottom respectively, after the indicated detrending and filtering processes.

Series corresponding to the experiments *3* and *8*, before and after the detrending and filter processes as indicated. Figure 6 presents the time series corresponding to experiments 3 and 8 after the indicated processes of detrending and filtering. Comparing Figures 3 and 6, it is possible to observe some apparently small changes in the corresponding times series however, in terms of information content, they are important and with strong implications to capture and model the potential chaotic content of them.

As can be seen in Figure 7 and Table 3 respectively, the time series appearance and chaos measures have some improvement after the detrending and denoising procedures. However, these improvements are not significative and even can have some negative impact regarding the objective of highlight the chaos content of the time series. This is because, as it was already mentioned before, the information of the chaotic behaviour of a time series is very delicate and distributed in a large range of low, medium and high frequencies.

Table 3

	Original time series			*Filtered time series*		
N_{Test}	τ	*Lyap*	*CD*	τ	*Lyap*	*CD*
3	*4*	*0.09*	*6.51*	*4*	*0.13*	*7.54*
8	*8*	*0.10*	*6.80*	*10*	*0.13*	*5.97*
	Detrended and then filtered time series			*Filtered and then detrended time series*		
	τ	*Lyap*	*CD*	τ	*Lyap*	*CD*
3	*4*	*0.11*	*7.80*	*4*	*0.11*	*7.75*
8	*9*	*0.12*	*7.03*	*9*	*0.12*	*6.77*

ISSN (Online) 2394-2320

International Journal of Engineering Research in Computer Science and Engineering (IJERCSE)

Vol 10, Issue 4, April 2023

Table 3. Chaos measures of the two time series corresponding to experiments 3 and 8, before and after the indicated detrending and filtering processes.

Therefore, the modelling process is applied to the time series corresponding to experiments *3* and *8*, before and after the detrending and noise filter processes. Since τ is a prescription value which depends on the size of the integration time step Δt, in each case the trajectory reconstruction is performed using $\Delta t \leq \tau \leq 200\Delta t$ obtaining two hundred possible 3D nonlinear models for each time series. Then each model is numerically integrated to obtain the *x* variable as a time series of data points to be compared with the original experimental time series, closing a feedback converging process between experimental information and nonlinear modelling information.

From this comparison process between experimental and numerical time series and their chaos content, we chose two cases that show a particularly interesting potential of chaotic dynamics. This does not mean that the dynamics of the other time series cannot be modelled by this method but, further analysis and tests have to be performed to improve the evidences of their potential of chaotic content. On the other hand, it is noteworthy that with optimized Δt numerical time series of 1500 data points, it would be easier to build nonlinear models of the possible chaotic behaviour of the PEMFCs with appropriated operation parameter values. This is a strong indication of the improvement or filtering power (detrending and denoising) of the modelling processes by itself. This is because, the self-consistency and robust information treatment that the modelling process performs in its different stages, largely and with accurate precision reduce the nonstationary and noise contamination of the time series without strong damage of the chaos information content of the time series.

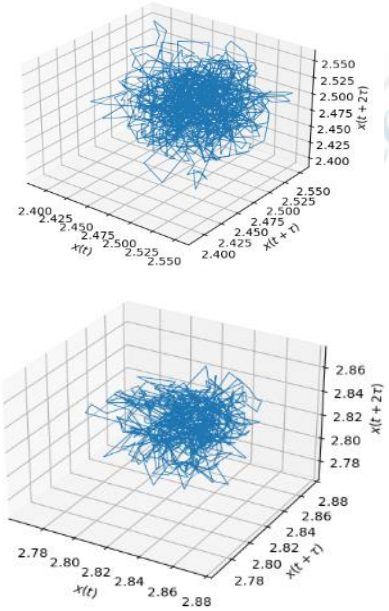

Figure 7

Figure 7: Reconstructed attractor from the voltage time series corresponding to N_{Test} = 3 (top), without any pre-processing for detrending or denoising and using a delay time τ = 120. Reconstructed attractor from the voltage time series corresponding to N_{Test} = 8 (Figure 7 bottom), without any pre-processing for detrending or denoising and using a delay time τ = 113.

The result of the reconstruction process is the numerical value of the coefficients of each term of the 3D dynamical system with nonlinearities up to order two, *i.e.* one constant, three linear terms and six nonlinear terms for each one of the three variables for a total of thirty coefficients. Tables 4 and 5 show the coefficients of the two models obtained from the time series corresponding to experiments 3 and 8 with delay times 120 and 113 respectively. In these two tables the three components $(\dot{x}, \dot{y}, \dot{z})$ represent the time derivatives of the 3D variables and the header of each column represents the coefficient of the corresponding combination of variables. This notation represents the function *F* in terms of polynomial terms that constitute the model as indicated in equation 2. The model is obtained by multiplying each variable by their respective coefficient. An example for the first line (corresponding to *x* as the first variable of the 3D dynamical system of differential equations), of Table 5 is shown in equation (7):

$$\dot{x} = -3.53 + 9.54x + 5.18y - 12.23z + 0.31x^2 - 3.67xy - 0.34xz + 0.95y^2 - 0.07yz + 2.37z^2 \quad (7)$$

The expressions corresponding to the $\dot{y}$ and $\dot{z}$ time derivatives are similarly written with the corresponding parameter values of the second and third lines from Table 5. The result, is a 3D dimensional model (3D autonomous nonlinear dynamical system of differential equations) defined by the values of the 30 corresponding coefficients. Similarly, it can be done for Table 4 corresponding to the experiment 3 and for any other model obtained from a time series of voltage data points.

It is evident that the numerical values of the coefficients of the models shown in tables 4 and 5 are totally different although they correspond to the same PEMFC but with different values of the operating parameters, indicating the sensitivity to initial conditions of the PEMFC and the model. This is the precise unpredictability of the PEMFC and its corresponding chaotic behaviour but at the same time the robustness and long-term predictability that the dynamics is kept in the attractor even under strong external influences.

Table 4

	c	x	y	z	x^2
$\dot{x}$	12,99	-8,95	0,71	-2,17	0,59
$\dot{y}$	14,07	5,12	-10,25	-6,13	-1,99
$\dot{z}$	-13,01	0,41	10,24	-0,12	0,29

ISSN (Online) 2394-2320

International Journal of Engineering Research in Computer Science and Engineering (IJERCSE)

Vol 10, Issue 4, April 2023

	xy	xz	y^2	yz	z^2
$\dot{x}$	2,27	0,12	-1	-0,56	0,66
$\dot{y}$	0,5	1,43	0,55	2,51	-0,73
$\dot{z}$	-0,4	-0,35	-2	0,27	0,06

Table 4. Coefficients of the 3D autonomous nonlinear dynamical system obtained from the time series corresponding to the experiment 3, using a delay time τ=120.

Table 5

	c	x	y	z	x^2
$\dot{x}$	-3.53	9.54	5.18	-12.23	0.31
$\dot{y}$	-1.13	-16.41	8.61	8.65	2.87
$\dot{z}$	2.94	9.37	-12.49	1.06	0.06
	xy	xz	y^2	yz	z^2
$\dot{x}$	-3.67	-0.34	0.95	-0.07	2.37
$\dot{y}$	-0.08	0.15	0.5	-3.98	0.39
$\dot{z}$	-0.57	-2.87	2.56	-0.12	1.3

Table 5. Coefficients of the 3D autonomous nonlinear dynamical system obtained from the time series of experiment 8, with delay time τ=113.

Table 6 shows the results of the chaos measures $\boldsymbol{\tau}$, *Lyap* and *CD* applied to the time series of the variable *x* obtained by numerical integration of the dynamical models obtained from the experimental time series corresponding to experiments 3 and 8 respectively. The values of τ are estimated with the mutual information and are the values used in the calculation of the other corresponding chaos measures. Therefore, it should be noted that these values of τ are not the same with which the models were constructed because they correspond to numerical time series where the chaos information is evident and the characteristics of the time series such as sampling frequency, Δt, detrending and denoising are numerically optimized and the modelling process implies a more precise and less disruptive filtering process as mentioned above. This can be seen in the results of the chaos measures more consistent with chaotic content and characteristics of the corresponding time series: the values of $\boldsymbol{\tau}$ are more consistent with the number and precision of the data points, the sampling frequency and Δt produced by the numerical integration, the values of *Lyap* are larger indicating more sensitivity to initial conditions as a landmark of chaos, and the values of the *CD* estimates are clearly fractal and between dimensions 2 and 3 as a clear indicator of a chaotic attractor. The filtering pre-processing to reduce tendencies (low frequency contamination), and white noise (high frequency contamination), improve significantly the results independently of the order of application of the two filtering processes. These results indicate that the modelling process has improved the proportion of the chaotic information content compared to other information contents of the experimental time series and also allows for a further improvement by means of simple and soft detrending and denoising pre-processing of the numerical time series.

Table 5

	Numerical time series			Filtered time series		
N_{Test}	$\boldsymbol{\tau}$	*Lyap*	*CD*	$\boldsymbol{\tau}$	*Lyap*	*CD*
3	23	0.30	2.38	5	0.21	2.52
8	25	0.22	2.05	10	0.30	2.60
	Detrended and then filtered time series			Filtered and then detrended time series		
3	5	0.19	2.14	5	0.18	2.14
8	8	0.23	2.40	8	0.23	2.42

Table 6. Chaos measures τ, *Lyap* and *CD* of the variable *x* integrated from the dynamical models from the experimental time series corresponding to the experiments *3* and *8* respectively. The values of τ are estimated with the mutual information function and these are the values used in the calculation of the other corresponding chaos measures.

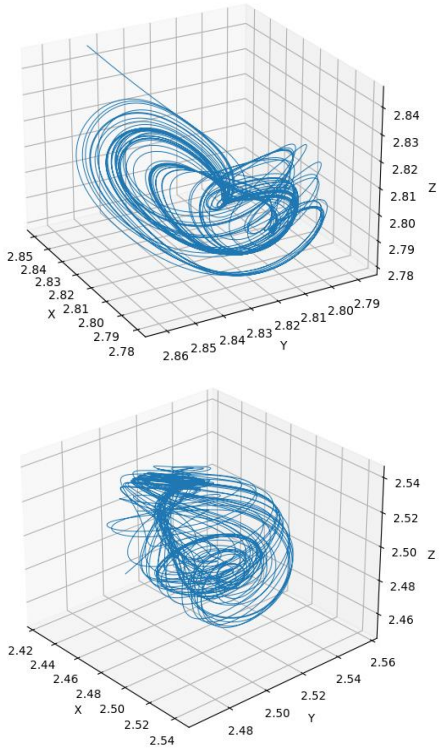

Figure 5: Attractors obtained from the integration of the models presented in tables 4 (top) and 5 (bottom). The numerical integration of the corresponding models was performed using the Runge-Kutta method with step h=0.001 and 10000 iterations.

Figure 5 shows the attractors obtained from the integration of the models represented in tables 3 and 4, using the Runge-Kutta method with step h = 0.001 and 10000 iterations. These attractors would indicate that the behaviour of the cell is confined within limits in phase space and the chaotic systems tend to remain confined within its attractor. In terms of control, it is possible that the cell acquires strong stability and robustness under perturbations and remains in the operational conditions of experiments 3 and 8.

V. CONCLUSION

The numerical analysis and modelling of experimental time series from PEMFC presented in this work show that there is an important potential of deterministic chaos contained in voltage time series of the PEMFC for certain operating conditions. These operating conditions can give to the PEMFC the robustness, stability, durability and efficiency corresponding to a nonlinear dynamical system with chaotic solution with an attractor of fractal dimension. The dynamical models developed in this process could provide new understanding and better control of the PEMFC that may increase further its stability, durability and efficiency.

The software developed and applied in this work, CMRTS (Chaotic Model Reconstruction from Time Series), allows an agile and efficient study and analysis of many different experimental time series obtained from diverse PEMFC operational conditions. It is therefore, a powerful tool for PEMFC research, development and even innovation towards a more efficient and competitive fuel cells.

The robustness of a chaotic behaviour in complex dynamic systems emerges from the tendency to keep the solution of the system, its trajectory in phase space, confined within an attractor for very long periods of time and resilient to relatively strong external persistent perturbations. Formally, it is a consequence of the energy distribution of a chaotic dynamic in a wide and continuous range of frequencies avoiding any destructive resonance which is always possible in complex dynamic systems. Therefore, this nonlinear modelling process could allow a different kind of control bringing the PEMFC through the operational parameters to a chaotic attractor resulting in a dynamical stability for long periods of time without the need of any other type of external control or additional energy expense. However, there is a lot of work to be done in order to develop better nonlinear dynamical models with the accuracy and fidelity needed to achieve the precise values of the operational parameters for each PEMFC, because they are very sensitive to any small variations of the materials and design of the different parts of the PEMFC. The automatization of the CMRTS and the new understanding of the PEMFC's dynamics that will provide the continuation of this R&D of nonlinear dynamical models applied to PEMFC, will also improve the diagnose and prevention of PEMFC failures and dysfunctional states, both on-line and off-line.

REFERENCES

[1] J. M. Thomas, "W.R. Grove and the fuel cell," Philos. Mag., vol. 92, no. 31, pp. 3757–3765, 2012, doi: 10.1080/14786435.2012.691216.

[2] M. A. Abdelkareem, K. Elsaid, T. Wilberforce, M. Kamil, E. T. Sayed, and A. Olabi, "Environmental aspects of fuel cells: A review," Sci. Total Environ., vol. 752, p. 141803, Jan. 2021, doi: 10.1016/j.scitotenv.2020.141803.

[3] PEM Fuel Cells. Elsevier, 2005.

[4] F. Barbir, PEM fuel cells: theory and practice, 2nd ed. Amsterdam ; Boston: Elsevier/Academic Press, 2013.

[5] R.M. Gutierrez, "Optimal nonlinear models from time series: an application to climate", Int. J. Bifurcation and Chaos, Vol. 14, No. 6 (2004) pp. 2041-2052.

[6] H.D.I. Abarbanel, "Analysisi of observed chaotic data", Springer, NY, 1996.

[7] J.C. Sprot, "Algebraicallysimple chaotic flows", Int. J. Chaos Th. Appl., Vol. 5, pp. 3-22.

[8] H. Kantz and T. Schreiber, "Nonlinear Time Series Analysis", 2nd edition, Cambridge University Press, Cambridge, 2004.

[9] The TISEAN software package, 2007, https://www.pks.mpg.de/tisean//Tisean_3.0.1/

[10] R.H. Enns and G.C. McGuire, "Nonlinear physics for scientists and engineers", Birkhauser, Boston, 1997.

[11] P. Glendinning, "Stability, instability and chaos: an introduction to the theory of nonlinear differential equations", Cambridge U Press, Cambridge, 1994.

[12] S.H. Strogatz, "Nonlinear Dynamics and Chaos: With Applications to Physics, Biology, Chemistry, and Engineering", Second Edition (Studies in Nonlinearity), CRC Press, 2014.

[13] R. Petrone et al., "A review on model-based diagnosis methodologies for PEMFCs," International Journal of Hydrogen Energy. 2013, doi: 10.1016/j.ijhydene.2013.03.106.

[14] Z. Zheng et al., "A review on non-model based diagnosis methodologies for PEM fuel cell stacks and systems," International Journal of Hydrogen Energy. 2013, doi: 10.1016/j.ijhydene.2013.04.007.

[15] A. Benmouna, M. Becherif, D. Depernet, F. Gustin, H. S. Ramadan, and S. Fukuhara, "Fault diagnosis methods for Proton Exchange Membrane Fuel Cell system," Int. J. Hydrogen Energy, vol. 42, no. 2, pp. 1534–1543, Jan. 2017, doi: 10.1016/J.IJHYDENE.2016.07.181.

[16] M. B. Burkholder, N. S. Siefert, and S. Litster, "Nonlinear analysis of voltage dynamics in a polymer electrolyte fuel cell due to two-phase channel flow," J. Power Sources, vol. 267, pp. 243–254, 2014, doi: 10.1016/j.jpowsour.2014.04.156.

[17] J.C. Robinson, "All possible chaotic dynamics can be approximated in three dimensions", Nonlinearity, 1998, Vol. 11, pp. 529-545.

[18] Y. Cao, Y. Li, G. Zhang, K. Jermsittiparsert, and M. Naseri, "An efficient terminal voltage control for {PEMFC} based on an improved version of whale optimization algorithm," Energy Reports, vol. 6, pp. 530–542, 2020, doi: 10.1016/j.egyr.2020.02.035.

[19] R. Mañe, "On the dimension of the compact invariant of certain nonlinear maps", in Dynamical Systems and

Turbulence, Lecture Notes in Mathematics, Vol. 898, Springer, Berlin, 1980, pp. 230-242.

[20] F. Takens, "Detecting strange attractors in turbulence", in Dynamical Systems and Turbulence, Lecture Notes in Mathematics, Vol. 898, Springer, Berlin, 1980, pp. 366-381.

[21] W. II. Press, S.A. Teukolsky, W.T. Vetterling and B.P. Planner, "Numerical Recipes, Cambridge U Press, NY, 1992.